

Semiclassical study of the collision of a highly excited Rydberg atom with the molecules HF and HCl

M. Kimura

*Argonne National Laboratory, Argonne, Illinois 60439
and Department of Physics, Rice University, Houston, Texas 77251*

N. F. Lane

Department of Physics, Rice Quantum Institute, Rice University, Houston, Texas 77251

(Received 26 January 1990)

The semiclassical impact-parameter method is applied to the processes of state changing and energy transfer in the collision of a highly excited Rydberg atom ($n \geq 20$) with the polar molecules HF and HCl. The relative motion of the molecule and atomic nucleus is taken to be rectilinear; the electron-molecule and ion core-molecule interactions are represented by cutoff dipole forms. Cross sections for transitions involving quantum numbers n and l of the atom and rotational quantum number j of the molecule are obtained for a range of collision energies and initial atomic and molecular states. Comparisons are made with the results of earlier classical studies and with the quantum-mechanical impulse approximation. Collision rates are calculated and compared with experimental values for l mixing and n and j changing. The agreement between experiment and theory is shown to be satisfactory, within the uncertainties of both the measurements and the theory. Cases of agreement and disagreement between various theories are examined. One finding of the present work is that the quantum-mechanical impulse approximation appears to significantly overestimate the values of various state-changing cross sections when the internal energy defect is small. The validity of the impulse approximation for collisions of Rydberg atoms with polar molecules is discussed.

I. INTRODUCTION

Highly excited Rydberg atoms continue to attract considerable attention by researchers interested in the response of these delicate atomic systems to external fields,¹ in their collision interactions² with atoms, molecules, ions, and surfaces, and recently in a study of quantum chaos.³ Whether the basic interest is in the dynamics of the Rydberg atom plus field (or plus collision target) system or simply in using the Rydberg atom as a probe of an intriguing environment,⁴ the possibilities for interesting physical phenomena are large in number and challenging to the theory. Studies of the interactions of Rydberg atoms with surfaces promise a whole new array of important discoveries.⁵

In an earlier study,⁶ hereafter referred to as study I, the classical Monte Carlo approach was applied to the collision of a Rydberg atom, treated as strictly hydrogenic, with polar molecules HF and HCl. It was felt that qualitatively reliable results could be expected from such an approach because the dynamics of the electron tends to be dominated by the Coulomb field, except for electron-molecule separations of about $200a_0$ or less, where the long-range dipole interaction becomes dominant. The primary goal of the work was to study the dependence of various cross sections (l mixing, n and j changing, ionization, and total quenching) on relative collision velocity, and initial values of quantum numbers n , l , and j . Further, by having control of the form and range of both the

electron-molecule and ion core-molecule interactions and the initial conditions on the trajectories, it was possible to examine the dynamics, at least the classical dynamics, in some detail.

The present study suggests that many of the results predicted by the classical study in I are qualitatively correct, although the classical results are not quantitatively accurate in a number of cases. Later in this paper, comparisons will be given to illustrate the degree of agreement with the new semiclassical results and with the measurements. In general, the classical results appear to predict the correct qualitative dependence of the various cross sections on relative collision velocity and on initial values of the quantum numbers. The classical rates for total quenching are qualitatively accurate. However, the classical l -mixing rates appear to be too small by a factor of $\frac{1}{2}$, and the classical j -changing rates are too small by factors of $\frac{1}{5}$ or less. The semiclassical rates are in much better agreement with the measured rates.⁷ Possible physical explanations will be advanced. A summary of some of the present results was given in an earlier joint theoretical-experimental paper.⁷

One rather fundamental result of the present work is the finding that the quantum-mechanical impulse approximation,⁸ which for sufficiently large n values appears to describe l -mixing collisions of Rydberg atoms with atoms⁹ and nonpolar¹⁰ or weakly polar¹¹ molecules, significantly overestimates the collision rates for various processes when the energy defect is small. The classical

study I suggested that, except for very large values of n (approximately $n > 70$), the impulse approximation will fail for Rydberg atom collisions with strongly polar molecules because of (i) the long-range nature of the dipole interaction, which dominates the collision dynamics, and (ii) the consequent increase in effective collision time due to multiple electron-molecule encounters that occur in a single collision. This situation is somewhat similar to that in ion-Rydberg atom collisions, where a simple impulse model based on the perturbation theory is not appropriate because of long-range Coulomb interaction.¹² An experimental demonstration that the impulse approximation fails, at least in the range of principal quantum numbers $24 < n < 49$, for collisions with NH_3 and ND_3 , has been provided by the Saclay group.¹³⁻¹⁵ In addition to the theoretical studies mentioned above for a molecular target, a recent investigation of ionization in $\text{Xe}(27f) + \text{HF}$ and $\text{Xe}(31f) + \text{HCl}$ collisions was reported by Shirai and Nakamura,¹⁶ in which the Born and Glauber approximations were employed. The authors reported calculated cross sections showing that the Glauber results were smaller than the Born results but provided no theoretical explanation of this difference. Although ionization is not included in the present study, what we have learned about the mechanisms that control electronic excitation and deexcitation suggests that a perturbation approach will not be valid for the range of initial quantum numbers considered here.

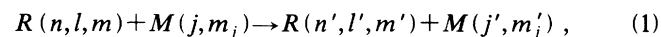
It is of interest to note that the semiclassical molecular-orbital (MO) expansion method has been applied to investigate total depopulation and l mixing to high l states in a collision of Rydberg $\text{Na}(n \geq 6)$ with He .¹⁷ This study shows that strong radial coupling at several avoided crossings provides the mechanism for a propensity rule for populating $l \geq 3$ states and appears to demonstrate the appropriateness of the MO approach to the Rydberg atom collision problem.

In Sec. II the theoretical approach will be described. In Sec. III the semiclassical results will be presented and compared with other theories and with the existing experimental measurements. A summary will be given in Sec. IV.

II. THEORY

The theoretical approach followed here is the standard semiclassical impact-parameter method¹⁸ used successfully in a large variety of heavy-particle collision problems, e.g., charge-transfer processes in intermediate-energy ion-atom collisions. This method is believed to be applicable here because only very large impact parameters are important to the processes studied, and the transfer of momentum and energy between the electron and the nuclei is not expected to play a significant role. We will return to these points later in the discussion.

The processes of interest in this investigation are



where R and M designate the Rydberg atom and molecule, respectively, with internal states specified by the usual quantum numbers. In the present study we are not

concerned with changes in m and m_j , so that all cross sections and collision rates will be defined in terms of averages over initial m and m_j and summation over final values of these quantum numbers.

The electronic energy of the Rydberg atom is defined by the Rydberg form (atomic units will be used throughout)

$$E_{n,l} = -\frac{1}{2}(n - \delta)^2, \quad (2)$$

where δ is the quantum defect. For Rb, the quantum defects are calculated to be 3.12, 2.64, 1.49, and 0.002 for $l=0, 1, 2,$ and 3 , respectively.¹⁹ For Xe, the respective values are 3.76, 3.35, 2.11, and 0.004.

The molecule is taken to be a simple rigid rotator, with rotational energy given by

$$E_j = B_j(j+1), \quad (3)$$

where the values of the rotational constant²⁰ B are 9.55×10^{-5} a.u. (20.95 cm^{-1}) for HF and 4.83×10^{-5} a.u. (10.59 cm^{-1}) for HCl.

In the semiclassical impact-parameter approach, the heavy-particle motion (i.e., the relative motion of the molecule and the ion core of the Rydberg atom) is taken to be classical. Since we are concentrating on phenomena in which the important interactions occur at large atom-molecule separations, the relative motion is taken to be rectilinear, so that

$$r_{\text{CM}} \equiv \mathbf{R} = \mathbf{v}t + \mathbf{b}, \quad (4)$$

where \mathbf{R} (r_{CM}) represents the position vector of the molecular center of mass relative to the ion core, \mathbf{v} is the relative velocity of the molecule with respect to the ion core, and \mathbf{b} is the impact parameter (see Fig. 1). With the relative heavy-particle motion taken to be classical, the Hamiltonian H reduces to that of the internal electronic motion of the atom and the rotational motion of the molecule; H is time dependent because the potential energy varies with time through \mathbf{R} according to Eq. (4). Thus, we have

$$H = H_e(\mathbf{r}) + H_m(\hat{\rho}) + V_{\text{EM}}(\mathbf{r}, \mathbf{R}, \hat{\rho}) + V_{\text{CM}}(\mathbf{R}, \hat{\rho}), \quad (5)$$

where H_e is the electronic Hamiltonian of the atom, H_m is the rotational Hamiltonian of the molecule, $\hat{\rho}$ is the orientation vector of the molecular axis, and V_{EM} and

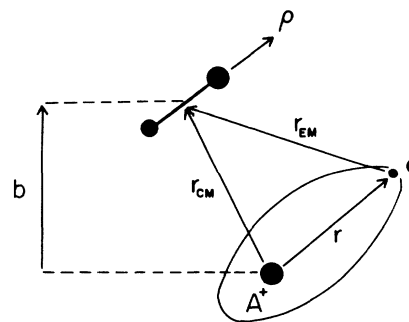


FIG. 1. Coordinates of Rydberg atom-molecule collision system.

V_{CM} are the electron-molecule and ion core-molecule interactions, respectively. As in the classical treatment I, we approximate these latter interactions by cutoff dipole forms,

$$V_{EM} = -e[(\mathbf{r}_{EM} \cdot \mathbf{d})/r_{EM}^3] \{1 - \exp[-(r_{EM}/r_0)^6]\}, \quad (6)$$

where r_{EM} is the molecule position vector relative to the electron and \mathbf{d} is the molecular dipole moment vector, with magnitude $d = 0.71ea_0$ (1.81×10^{18} esu) for HF and $0.42ea_0$ (1.08×10^{18} esu) for HCl. The second factor removes the unphysical singularity at $r_{EM} = 0$ by means of the cutoff factor, with cutoff radius r_0 . A similar form is used for the interaction between the ion core and the molecule, but with $-e$ and \mathbf{r}_{CM} substituted for e and \mathbf{r}_{EM} , respectively. The simple forms chosen here are identical to those used in the classical treatment in I and can be justified in part by the results of quantum-mechanical calculations of electron-molecule scattering by using the cutoff dipole form as well as more accurate interactions.²¹ The classical study described in I showed that the cross sections were insensitive to the values of the cutoff radius for values $0.5a_0 < r_0 < 4a_0$; similar insensitivity has been found in the present calculations.

The system is described by a time-dependent wave function satisfying the Schrödinger equation

$$i \frac{\partial \Psi}{\partial t} = H \Psi, \quad (7)$$

where the Hamiltonian is given by Eq. (5). In the usual manner, the wave function is represented by an expansion in terms of internal system energy eigenfunctions, i.e., products of Rydberg atomic orbitals times molecular rotational eigenfunctions. In the present treatment, however, we have employed adiabatic perturbed rotating molecule (PRM) eigenfunctions²² rather than the usual unperturbed rotational eigenfunctions because the PRM expansion gives faster convergence than that of the conventional rotational states. Thus, the expansion takes the form

$$\Psi = \sum_i a_i(t) \phi_i^{AO}(\mathbf{r}, t) X_i^{PRM}(\mathbf{r}_{EM}, \hat{\rho}), \quad (8)$$

where ϕ_i^{AO} are the Rydberg atomic orbitals (AO) with appropriate phase factors, X_i^{PRM} are PRM functions described below, and the coefficients $a_i(t)$ correspond to the transition amplitudes in the limit $t \rightarrow +\infty$.

The Rydberg atomic orbitals are approximated by Slater-type orbitals (STO's), which are nodeless and thereby result in much simpler radial integration in calculating the matrix elements that arise in the treatment. The positions of the STO radial maxima have been ad-

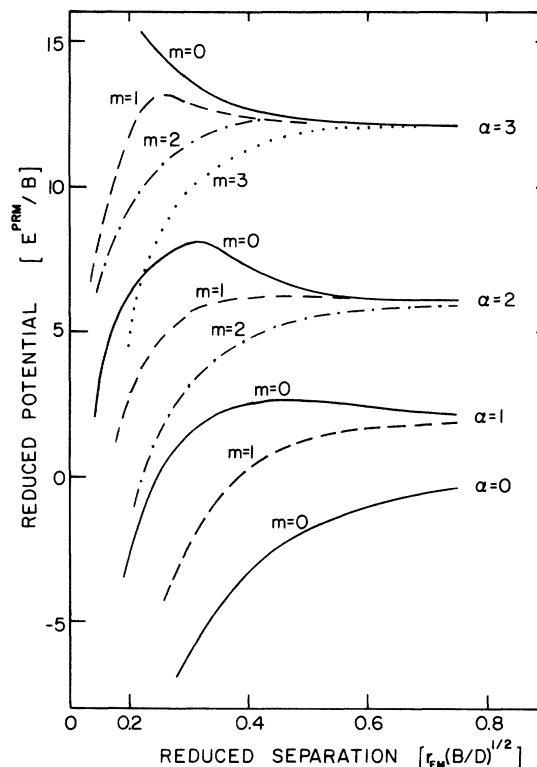


FIG. 2. Adiabatic potentials of perturbed rotating states as a function of separations [both in reduced units E^{PRM}/B vs $r_{EM}(B/D)^{1/2}$ where B and D are the rotational constant and the dipole moment of the molecule].

justed by using the proper quantum defect for each state. The error in the matrix elements due to this approximation is estimated to be $\sim 10\%$. (A test was carried out in the exact hydrogenic wave functions.)

The PRM functions are eigenfunctions of the rotational Hamiltonian of the molecule perturbed by the field of a stationary electron located at a distance r_{EM} away [the second and third terms in Eq. (5)]. The adiabatic eigenvalues of this Hamiltonian are, of course, simply the Stark-shifted rotational energies. These are illustrated in Fig. 2 for HF and HCl, in reduced units. These adiabatic PRM states are coupled by the relative motion of the electron with respect to the molecule, the coupling being particularly strong in the vicinity of avoided crossings, and by the core-molecule interaction.

Substitution of the expansion in Eq. (8) into the Schrödinger equation (7) yields the usual set of first-order, coupled equations,

$$\begin{aligned} i\dot{a}_{J\lambda}(t) = & \epsilon_{\lambda} a_{J\lambda}(t) + \sum_{J,\lambda} \langle \phi_{\lambda}^{AO}(\mathbf{r}, t) | E_{JM}(\mathbf{r}_{EM}) | \phi_{\lambda}^{AO}(\mathbf{r}, t) \rangle \delta_{J'M'JM} a_{J\lambda}(t) \\ & + \sum_J \langle X_{J'M'}^{PRM}(\mathbf{r}_{EM}, \theta', \phi') | V_{CM} | X_{JM}^{PRM}(\mathbf{r}_{EM}, \theta', \phi') \rangle \delta_{\lambda'\lambda} a_{J\lambda}(t) \\ & - i \left[\sum_{J\lambda} \left\langle X_{J'M'}^{PRM}(\mathbf{r}_{EM}, \theta', \phi') \phi_{\lambda'}^{AO}(\mathbf{r}, t) \left| \frac{\partial}{\partial t} \right| X_{JM}^{PRM}(\mathbf{r}_{EM}, \theta', \phi') \phi_{\lambda}^{AO}(\mathbf{r}, t) \right\rangle \right] a_{J\lambda}, \end{aligned} \quad (9)$$

where $\lambda=(n,l,m)$ represents quantum numbers of the Rydberg atom. The third term on the right-hand side represents the core coupling that induces rotational excitation-deexcitation of the molecule, while the last term is the nonadiabatic coupling that causes both electronic and rotational transitions for the Rydberg atom and molecule, respectively. Note that nonadiabatic couplings in the fourth term for the electronic states involve angular coupling *only* and consequently give rise to the $m \rightarrow m \pm 1$ transition selection rule.

The coupled equations (9) are solved numerically subject to the initial conditions

$$a_i(-\infty) = \delta_{ij} . \quad (10)$$

The cross sections are obtained by integrating the absolute squares of the transition amplitudes for the m th channel $P_m(b,E) = |a_m(+\infty)|^2$ over all impact parameters according to the relation

$$\sigma_m = 2\pi \int_0^\infty b db P_m(b,E) . \quad (11)$$

This form assumes cylindrical symmetry for the transition amplitudes, which is appropriate in the present application because important collisions take place at large internuclear separations, i.e., $b \gg \rho$. The range of impact parameters required in Eq. (9) depends on the Rydberg atom quantum numbers n, l of the initial and final states. For example, for the transition $40s \rightarrow 41p$, impact parameters up to $\sim 2000a_0$ were required. Straight-line trajectories were employed for the heavy-particle motion. This assumption is justified by the small fraction of momentum that is transferred between the electron and nuclei. It is interesting to compare Eq. (9) with that obtained from the impulse approximation (IA).⁹ If one neglects all terms on the right-hand side except the last and drops the summation (i.e., retains only the initial state), one recovers the IA (Ref. 9) within an impact-parameter description. Further discussions on this point will be deferred to Sec. IV.

The major source of numerical uncertainty in the present approach is the rate of convergence of the

coupled-states expansion in Eq. (9). Since the density of Rydberg states is high and the energy level separation small, in the range of initial and final states of interest, one might expect that many states would be strongly coupled and therefore that the expansion would converge very slowly. It turns out, however, that convergence can be obtained with a tolerable error, estimated at about 25%, with a modestly sized basis. We will return to this question in Sec. III, where we will present data on the convergence. For most of the calculations reported in Sec. III, we have used 15 PRM functions and all (l,m) atomic orbitals corresponding to 18 values of the principal quantum number n , thus giving rise to a total of about 350 channels for cases with large n ($n=40$) and somewhat less for cases with small n ($n=20$). Larger basis sets were used to estimate the accuracy of the calculations. Representative orbitals used are given in Table I.

III. RESULTS AND DISCUSSION

In our earlier classical studies, reported in I, cross sections for l mixing, n changing, j changing, and ionization were calculated for a range of relative velocities and initial values of all the quantum numbers. We have not attempted to repeat all of these studies with the semiclassical approach. Rather, we have carried out the calculations required to test the accuracy of the classical results and to compare with experimental results, including data obtained since the classical results were published.

In Fig. 3 the cross sections for n changing are illustrated for a collision of Xe($25d$) with HF($j=2$) for a range of final principal quantum numbers n' . The semiclassical cross sections, scaled downward by a factor of $1/(1.7)$ are shown as triangles and the earlier classical Monte Carlo results as bars, where the height of the bar denotes the statistical error in bin assignment of the Monte Carlo calculation. Thus, the first point to make in the comparison is that the semiclassical cross sections that include l mix-

TABLE I. Rb($40s$) + HF.

(i) Atomic orbital (AO) of Rb($40s$)	
(a) Region I ($R \leq 2000a_0$)	
n :	30–48
l :	0–15
m :	0–10
Total:	355 AO's
(b) Region II ($R > 2000a_0$)	
n :	30–45
l :	0–10
m :	0–5
Total:	185 AO's
(ii) Perturbed rotating molecule (PRM) state of HF	
α :	0–15
m :	0–10
Total:	55 PRM's

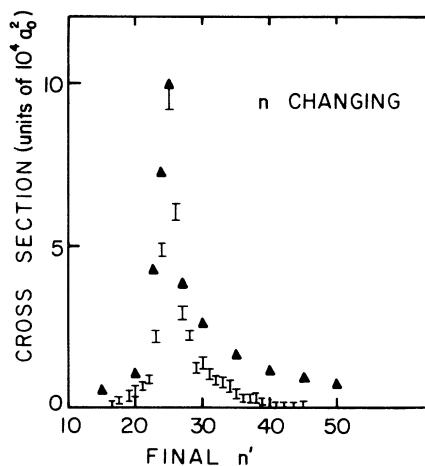


FIG. 3. n -changing cross sections in Xe**($25d$) + HF($j=2$) collisions. \blacktriangle , present work (semiclassical, scaled down by $1/1.7$); I, Ref. 6 (classical).

ing are larger than the classical results by a factor of nearly 2 at $n'=25$ and more at larger values of n' ; hence, it immediately follows that the semiclassical l -mixing rates, at least for this case, are in better agreement with experiment.²³ The theoretical and experimental rates will be compared later in this section. The factor-of-2 difference in the absolute value of the classical l -mixing cross section is not particularly troubling, since the classical results were at most expected to provide a qualitative description of these complex collision processes. However, we believed that a test should be made of the dependence of the cross section on initial quantum numbers and have carried out such a set of semiclassical calculations for the l -mixing cross sections for a range in values of initial principal quantum numbers n .

In Fig. 4 semiclassical and classical l -mixing cross sections are compared for collisions of $\text{Xe}(nd)$ with $\text{HF}(j=2)$. The semiclassical cross sections are reduced by the factor $1/(1.8)$. Except at very high values of n ($n > 80$), the n dependence is well represented by the classical results. One significant deficiency of the classical treatment is the lack of energy quantization for either the electronic states of the Rydberg atom or the rotational states of the molecule. Hence, any sensitivity of the cross sections to the total system energy defect will be missed in the classical treatment. Indeed, the energy defect can classically be zero in all cases, i.e., arbitrary amounts of energy can be transferred between the atomic electron and the molecule. In the semiclassical treatment, energy quantization is properly included.

In Fig. 5 the semiclassical n -changing cross sections for collisions of $\text{Rb}(49s)$ with $\text{HF}(j=1)$ are illustrated for a range of final principal quantum numbers n' . For n' slightly large or slightly smaller than the initial value $n=49$, the cross sections are still quite large. (For example, the value at $n'=70$ is still about 20% of the peak value, even though this transition corresponds to an energy defect of about 20 cm^{-1} .) As n' becomes much smaller than 49, the cross section falls rapidly, primarily because of the large energy defect required for the transition. The cross section for the "upward" transition also falls off with increasing n' . However, in the vicinity of $n'=100$, the cross section rises through a maximum before falling again at higher n' . By examining the value of

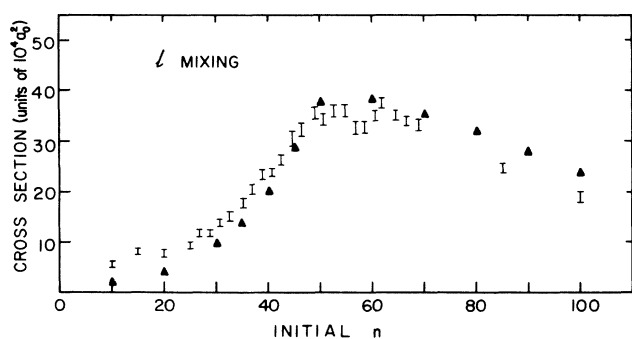


FIG. 4. l -mixing cross sections in $\text{Xe}^{**}(nd) + \text{HF}(j=2)$ collisions. \blacktriangle , present work (semiclassical, scaled down by $1/1.8$); I, Ref. 6 (classical).

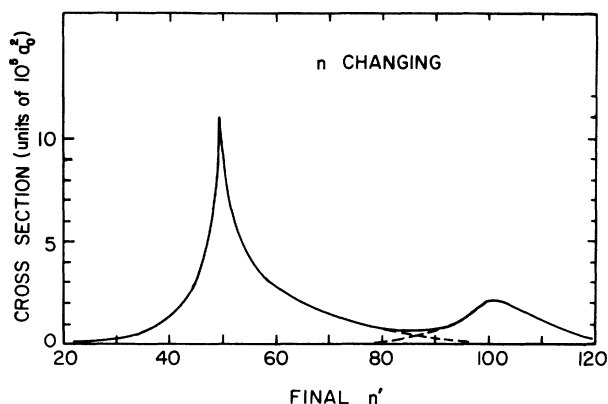


FIG. 5. n -changing cross sections in $\text{Rb}^{**}(49s) + \text{HF}(j=1)$ collisions.

the final rotational quantum number j' , one sees that the hump about $n'=100$ results from a simultaneous rotational deexcitation transition, so that the total energy defect is small. This qualitative effect was obtained by Matsuzawa in his early theoretical studies based on the quantum-mechanical impulse approximation^{24,25} and has been experimentally observed as a regular feature of selective field ionization (SFI) spectra from the earliest measurements.²³

It is interesting to compare the two peaks in the n -changing cross section. If one arbitrarily defines the boundary of each peak as the n' value where the cross section has fallen to 20% of the respective peak value, then the principal peak (that centered around $n'-n=49$) is about 20 cm^{-1} wide, as noted earlier. However, with the same definition of the boundary of the $j'=j-1=0$ peak (around $n'=100$), one finds that peak to be about 4 cm^{-1} in width. One possible explanation of this observation is that the effective collision time is shorter for collisions in which n is changed by small amounts and j not at all, than for collisions where n changes by a large amount but is accompanied by a simultaneous change of j by 1. The "Massey criterion," based on the Heisenberg uncertainty principle,²⁶ would suggest that the shorter collision time would permit the larger energy defect. The reason for the different effective collision times in the two cases is simply that the long-range inverse-square dipole interaction is involved (to first order) when the rotational quantum number changes by one. However, the rotationally elastic processes, where n changes by a small amount, is dominated by a shorter-range interaction consisting of the second-order contribution from the dipole potential, which (in second order) falls off asymptotically as r^{-4} , and by other contributions of equal or shorter range.

Comparison with the experimental measurements is complicated by the fact that only collision rates are measured; moreover, precise state-to-state rates are not available. When the cross section is independent of velocity, the collision rate k is defined in terms of the cross section by the expression

$$k = \sigma \bar{v}, \quad (12)$$

TABLE II. Rotational deexcitation.

Rate const. k (10^{-7} cm ³ /s)	Expt. (Ref. 24)	Classical (Ref. 6)	Present work
(i) Xe(27f)+HF			
$k(j=2 \rightarrow 1)$	3.0 (± 1.5)	0.75 (± 0.07)	2.1
$k(j=3 \rightarrow 2)$	2.2 (± 1.1)	0.34 (± 0.003)	1.6
(ii) Xe(31f)+HCl			
$k(j=2 \rightarrow 1)$		0.35 (± 0.04)	1.4
$k(j=3 \rightarrow 2)$		0.35 (± 0.04)	1.3

where \bar{v} is the average relative velocity (the speed) of the molecule with respect to the Rydberg atom. In Table II the measured rates^{23(a),23(b)} for rotational deexcitation in collisions of Xe Rydberg atoms with HF molecules are compared with the theoretical rates determined by the classical Monte Carlo and semiclassical methods. (Theoretical rates are given for the case of HCl, as well.) As anticipated from the comparison of the theoretical cross sections in Fig. 3, the semiclassical rates are much larger than the classical values and in good agreement with the measurements. This improvement is in part attributable to inclusion in the present calculation of the core-molecule interaction, V_{CM} , which contributes significantly to j changing.

Experimental rates for rotational deexcitation of HF in collisions with Rb Rydberg atoms^{23(c),23(d)} and corresponding excitation of the Rydberg electron (i.e., upward transitions) are compared with the semiclassical rates in Fig. 6 for a range of initial principal quantum numbers n . The agreement is satisfactory and is much better than that of the quantum-mechanical impulse approximation, also shown for comparison.²⁷ It is important to note that in the case of upward transitions, the final electronic density of states is sufficiently high and the corresponding energy-level separation sufficiently small so that a nearly exact energy match is always possible. (The specific rates are given in Table III.) Thus, it is not surprising that the dependence on n is slight, in fact not discernible within this range of n values. We have also performed calculations for lower Rydberg Rb($n=20$)+HF collisions and

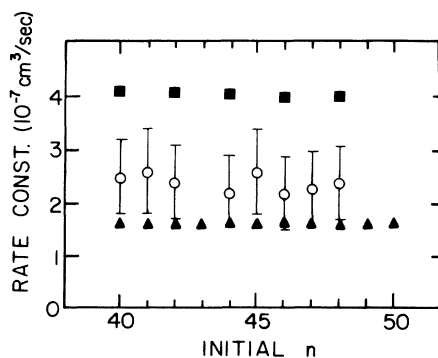


FIG. 6. Upward transition rates in Rb^{**}(ns)+HF($j=1$) collisions. ■, Ref. 27 (impulse approximation theoretical results); ▲, present work (semiclassical theoretical results); ○, Ref. 28 (experimental results).

find that the general trends discussed for higher Rydberg Rb($n \geq 46$)+HF collisions hold but that the magnitudes of the cross sections for the former are smaller because of larger energy defects for the lower states.

The situation is somewhat different for the rates corresponding to rotational excitation, which are accompanied by deexcitation of the Rydberg electron (i.e., “downward” transitions). In these cases, transitions can be selected that have defects ranging from nearly zero to about 3.5 cm⁻¹. In Fig. 7 and Table IV the measured rates²³ are compared with theoretical rates calculated by using the semiclassical approach or the quantum-mechanical impulse approximation.²⁷ One can see that all rates fall off with increasing energy defect ΔE , as one might expect from the Massey criterion.²⁶ However, it appears that the true dependence on ΔE is far less than that predicted by the quantum-mechanical impulse approximation.²⁷ Petitjean *et al.*¹³⁻¹⁵ also noted that the IA appears to overestimate the cross sections for state changing in NH₃ and ND₃. Referring again to Fig. 7, we see that the agreement between the experimental and theoretical semiclassical rates appears to be satisfactory.

The earlier classical Monte Carlo calculations⁶ showed a significant increase in the rotational excitation and deexcitation cross sections with respect to increasing initial angular momentum l of the Rydberg electron. The semiclassical calculations confirm this prediction. It may be worthwhile to point out that at large n (≥ 30), the Rb(ns) levels are nearly degenerate with those of Rb[($n-3$), $l \geq 3$], since the quantum defect is 3.12. Therefore, the downward transition tends to populate

TABLE III. Rb^{**}(nl)+HF($j=0$ or 1) collisions.

nl	n upward ($j=1 \rightarrow 0$) (10^{-7} cm ³ /s)	
	Experiment (Ref. 28)	Present work
40s	2.5 \pm 0.7	1.616
41s	2.6 \pm 0.8	1.635
42s	2.4 \pm 0.7	1.614
43s		1.617
44s	2.2 \pm 0.7	1.621
45s	2.6 \pm 0.8	1.619
46s	2.2 \pm 0.7	1.617
47s	2.3 \pm 0.7	1.620
48s	2.4 \pm 0.7	1.622
49s		1.638

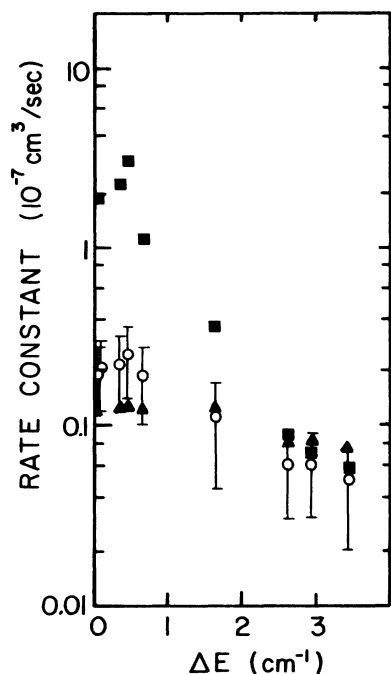


FIG. 7. Downward transition rates in $\text{Rb}^{**}(ns)+\text{HF}(j=0)$ collisions. ■, Ref. 27 (impulse approximation theoretical results); ▲, present work (semiclassical theoretical results); ○, Ref. 28 (experimental results).

different n' levels with a wide range of high l values but not necessarily the $l < 2$ levels. A similar finding has been reported for l changing in the Na^{**}/He collision system based on an application of the molecular-orbital expansion method.¹⁷ Furthermore, because of the strong rotational coupling that connects different m states, as described in coupled Eq. (9), large m -changing transitions through a series of rotational couplings are favorable, although the probability is not large. This observation is consistent with the results of the IA.²⁸

Semiclassical rates for upward transitions in collisions of $\text{Rb}(49l)$ with $\text{HF}(j=1)$ molecules are given in Table V for initial s , p , d , and f states. The rate increases by a factor of 2 across the sequence. This is because the more diffuse nature of the wave function with higher l is re-

TABLE IV. $\text{Rb}^{**}(nl)+\text{HF}(j=0 \text{ or } 1)$ collisions.

nl	n downward ($j=0 \rightarrow 1$) ($10^{-8} \text{ cm}^3/\text{s}$)	
	Experiment (Ref. 28)	Present work
40s	2.1 ± 0.9	1.142
41s	0.5 ± 0.3	0.732
42s	2.5 ± 1.1	1.234
43s		1.199
44s	2.2 ± 1.0	1.287
45s	0.6 ± 0.3	0.814
46s	1.9 ± 0.9	1.208
47s	0.6 ± 0.3	0.787
48s	1.9 ± 0.9	1.189
49s		1.172

TABLE V. $\text{Rb}^{**}(nl)+\text{HF}(j=0 \text{ or } 1)$ collisions: l dependence of n -upward rate constants.

Initial nl	n upward ($j=1 \rightarrow 0$) ($10^{-7} \text{ cm}^3/\text{s}$)
	Present work
49s	1.6
49p	2.1
49d	2.8
49f	3.1

sponsible for the transition. Both the qualitative trend and magnitude of the effect are in harmony with experimental measurements.²⁹

The tendency for the quantum-mechanical impulse approximation to overestimate the cross sections and the corresponding rates for the processes under discussion here is consistent with earlier observations. In numerous applications of the impulse approximation to l mixing in collisions of Rydberg atoms with other atoms, the IA consistently overestimated the cross section at small values of initial principal quantum number.^{2,9} In a formal expansion of the total system t matrix,⁸ the IA corresponded to retaining only terms up to the first order in the electron-atom (molecule) or the ion core-atom (molecule) scattering. At sufficiently high n , higher-order correction terms neglected in the IA were shown to be small.⁸ At small n , explicit inclusion of selected higher-order terms, specifically those that account for the attractive electron interaction with the ion core, was shown to reduce significantly the magnitudes of the cross sections.³⁰

We are not aware of a precise way of determining *ab initio* where the IA will fail. However, in the case of l -mixing collisions with atoms, it appears that the IA begins to fail just beyond the maximum that appears in all the curves describing the l -mixing cross section as a function of initial n . The maximum appears to shift to higher n for more strongly interacting atoms, i.e., in the target sequence He, Ne, Ar, Kr, Xe.^{2,9} Thus Fig. 4 suggests

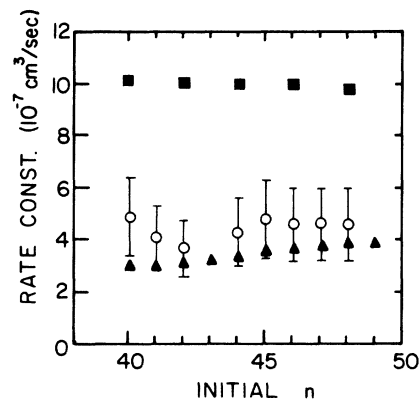


FIG. 8. l -mixing rates in $\text{Rb}^{**}(ns)+\text{HF}(j=1)$ collisions. ■, Ref. 27 (impulse approximation theoretical results); ▲, present work (semiclassical theoretical results); ○, Ref. 28 (experimental results).

TABLE VI. Rb^{**}(*nl*)+HF(*j*=1) collisions.

<i>nl</i>	<i>l</i> mixing (10 ⁻⁷ cm ³ /s)	
	Experiment (Ref. 28)	Present work
40s	4.9±1.5	2.765
41s	4.1±1.2	2.887
42s	3.7±1.1	3.105
43s		3.234
44s	4.3±1.3	3.309
45s	4.8±1.5	3.521
46s	4.6±1.4	3.678
47s	4.6±1.4	3.728
48s	4.6±1.4	3.803
49s		3.980

that the IA is likely to fail for *n* less than about 50 to 60 for collisions of Xe(*nd*) atoms with HF(*j*=2) molecules. It is interesting to note that the classical Monte Carlo results⁶ predict this because they seem to exhibit the correct shape of the variation of the cross sections with respect to *n*. In some sense, a fairly strongly polar molecular such as HF behaves like a strongly interacting, highly polarizable atom (e.g., Rb), at least in *l*-mixing collision processes.

In Fig. 8 and Table VI measured rates²³ for *l*-mixing in collisions of Rb Rydberg atoms with HF molecules are compared with the results of the semiclassical and quantum-mechanical impulse approximations.²⁷ It should be noted that the application of the IA to *l* mixing for polar molecules, using the usual first Born approximation for the electron-molecule scattering amplitude, is particularly inappropriate. In fact, *l* mixing occurs primarily through "elastic" electron-molecule scattering, where the dipole interaction does not enter to the first order and where shorter-range interactions thus dominate.²¹ Once again, the present semiclassical results are in good agreement with experiment.

We should emphasize that even if the electron-

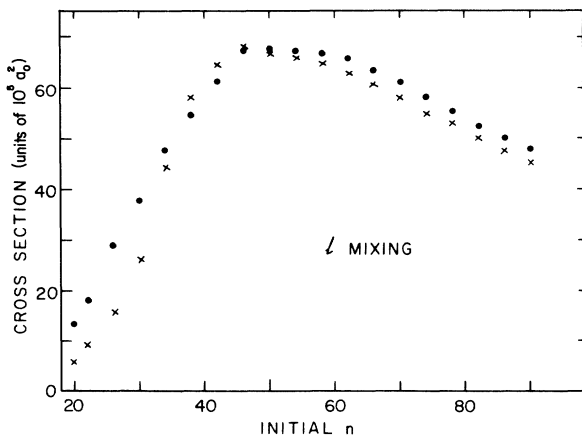


FIG. 9. *l*-mixing cross sections in Rb^{**}(*ns*)+HF(*j*=1) collisions. Expansion bases are ●, 7 α PRM + 5*n* AO; ×, 15 α PRM + 15*n* AO.

molecule scattering contribution to the IA amplitude were to be properly included, the IA would probably fail for the values of *n* included in Fig. 8 because the higher-order correction terms that are missing in the IA are also likely to be important. This can be seen in Fig. 9, where the *l*-mixing cross sections for Rb(*ns*) in collisions with HF(*j*=1) are plotted against initial *n*. The occurrence of the peak in the region 40 < *n* < 60 suggest that the IA will fail for *n* below 50 or 60. In Fig. 9 we also show the sensitivity of our calculated cross sections to the size of the PRM and atomic orbital (AO) basis set used in the expansion of the wave function. The larger basis set was used for all the rate calculations reported in this paper. For the lower Rydberg [Rb(*n* \geq 20)+HF] case, the general trends described above are again found to be the same, except, of course, for the magnitudes of the cross sections.

IV. SUMMARY AND CONCLUSIONS

We have carried out semiclassical, close-coupling calculations in order to study the transfer of internal energy and angular momentum in the collisions of highly excited atoms of Rb and Xe with the polar molecules HF and HCl by using basis sets consisting of 150–400 terms. The present semiclassical results show improvement over the classical treatment⁶ and give reasonably good agreement with measurements⁷ of *n*-upward, *n*-downward, *l*-mixing, and rotational deexcitation rates at thermal energies. Several test calculations were carried out to examine the sensitivity of the cross sections to the size of the basis sets and to the respective contributions of particular terms in the coupled Eq. (9). Of course, the most important terms for inelastic transitions are the third (core-molecule coupling) and fourth (electronic-rotational coupling). The third term in Eq. (9) describes rotational excitation-deexcitation through the core-molecule interaction; this, in turn, feeds back to influence the Rydberg electron. Thus, the third term plays the role of a higher-order correction to the IA. We carried out two sets of calculations, with and without inclusion of the third term of the cross section for *l* mixing in Xe(50*d*)+HF collisions. Neglecting the third term was found to decrease the magnitude of the *l*-mixing cross section by about 35% but the overall *n* dependence was not so affected. Inclusion of the core-molecule interaction tends to "orient" the molecular axis because of long-range core-molecule dipole interaction and consequently makes *l* mixing more efficient since molecular rotation, which tends to average out the electron-molecule dipole interaction, is hindered (by the orienting field of the ion core). General tests of the basis size have been carried out by using (i) a different number of *n* state with fixed *l* and *m* values, (ii) a different number of *l* states with fixed *n* and *m* values, and (iii) a different number of *m* states with fixed *n* and *l* values. A fairly small portion of the probability shifts around within a given *n*, *l*, and *m* space, so that a change in the number of *n*, *l*, and *m* states in the close-coupling calculation can cause differences as large as 25% in particular cross sections. After an initial distribution of probability in *n*, *l*, and *m* substates is established by the interaction

on the incoming trajectory (within a typical interaction region of $\sim 200a_0$), the probability rather quickly selects a certain set (or window) of dominant final states resulting from the quenching, i.e., "a quenching window." Further probability redistribution among different l and m substates on the outgoing trajectory is a slow and inefficient process that results from the long-range dipole interaction at very large atom-molecule distances.

The IA results obtained by using formulae of Petitjean and Gounand²⁷ appear to overestimate most of the reaction rates. The IA is derived on the basis of assumptions of (i) $r \gg r_{EM}$, (ii) $r \gg R$, (iii) no multiple scattering, (iv) neglect of V_{CM} , (v) weak binding energy of the Rydberg electron, and (vi) smooth binding potential. In the present Rydberg atom-polar molecule collisions, conditions (i)–(iii) are not met in any strict sense for $n \lesssim 50$, and there is no justification for condition (iv). However, several earlier studies carried out on the quenching of Rydberg atoms in collisions with polar molecules, which were based on the IA method, seemed to suggest that the IA offers a reasonable result for rather low n ($n \approx 20$) Rydberg atom collisions. Since these latter studies tended to emphasize transitions with rather large system ener-

gy defects and consequently short effective collision times, the IA may have some validity.

Lastly, it should be emphasized that in the present close-coupling scheme, ionization channels were excluded, and as is known from extensive studies of "high-energy" heavy-particle collisions,³¹ the neglect of continuum states usually results in an overestimation of discrete inelastic transition probabilities. However, considering the magnitude of the measured ionization cross sections for the present systems, we estimate that our calculated cross sections may be overestimated by 4–5%, at most, because of this effect.

ACKNOWLEDGMENTS

This work was supported in part by the U.S. Department of Energy, Assistant Secretary for Energy Research, Office of Health and Environmental Research, under Contract No. W-31-109-Eng-38 (M.K.); Office of Basic Energy Sciences, Division of Chemical Sciences (N.F.L.); and by the Robert A. Welch Foundation (N.F.L.)

- ¹T. F. Gallagher, in *In Rydberg States of Atoms and Molecules*, edited by R. F. Stebbings and F. B. Dunning (Cambridge University, Cambridge, 1983), p. 165.
- ²F. B. Dunning and R. F. Stebbings, in *In Rydberg States of Atoms and Molecules*, edited by R. F. Stebbings and F. B. Dunning (Cambridge University, Cambridge, 1983), p. 315.
- ³G. R. Welch, M. M. Kash, C. H. Iu, L. Hsu, and D. Kleppner, *Phys. Rev. Lett.* **62**, 1975 (1989).
- ⁴D. Kleppner, M. G. Littman, and M. L. Zimmerman, in *In Rydberg States of Atoms and Molecules*, edited by R. F. Stebbings and F. B. Dunning (Cambridge University, Cambridge, 1983), p. 73.
- ⁵F. B. Dunning, C. Rau, and G. K. Waters, *Comments Solid State Phys.* **12**, 17 (1985).
- ⁶S. Preston and N. F. Lane, *Phys. Rev. A* **33**, 148 (1986).
- ⁷A. Kalamarides, L. N. Goeller, K. A. Smith, F. B. Dunning, M. Kimura, and N. F. Lane, *Phys. Rev. A* **36**, 3108 (1987).
- ⁸M. Matsuzawa, *J. Phys. B* **17**, 795 (1984).
- ⁹M. Matsuzawa, *J. Phys. B* **12**, 3743 (1979).
- ¹⁰M. R. Flannery, *Ann. Phys. (N.Y.)* **79**, 480 (1973).
- ¹¹E. de Prunele and J. Pascale, *J. Phys. B* **12**, 2511 (1979).
- ¹²K. B. McAdam, *Phys. Rev. A* **34**, 2767 (1986).
- ¹³L. Petitjean, F. Gounand, and P. R. Fournier, *Phys. Rev. A* **30**, 71 (1984).
- ¹⁴L. Petitjean, F. Gounand, and P. R. Fournier, *Phys. Rev. A* **33**, 143 (1986).
- ¹⁵L. Petitjean, F. Gounand, and P. R. Fournier, *Phys. Rev. A* **33**, 1372 (1986).
- ¹⁶T. Shirai and H. Nakamura, *Phys. Rev. A* **36**, 4290 (1987).
- ¹⁷A. Kumar, N. F. Lane, and M. Kimura, *Phys. Rev. A* **39**, 1020 (1989).
- ¹⁸M. R. C. McDowell and J. P. Coleman, *Introduction to the Theory of Ion-Atom Collisions* (North-Holland, Amsterdam, 1970).
- ¹⁹C. E. Theodosiou, M. Inokuti, and S. T. Manson, *At. Data Nucl. Data Tables* **35**, 473 (1986).
- ²⁰K. P. Huber and G. Herzberg, *Molecular Spectra and Molecular Structure* (Van Nostrand, New York, 1979).
- ²¹N. F. Lane, *Rev. Mod. Phys.* **52**, 29 (1980); see discussion pp. 103–107.
- ²²The basic ideas of the PRM is similar to the perturbed stationary state (PSS) method in heavy-particle collision. See the PSS in Ref. 18.
- ²³(a) K. A. Smith, F. G. Kellert, R. D. Rundel, F. B. Dunning, and R. F. Stebbings, *Phys. Rev. Lett.* **40**, 1362 (1978); (b) F. G. Kellert, K. A. Smith, R. D. Rundel, F. B. Dunning, and R. F. Stebbings, *J. Chem. Phys.* **72**, 3179 (1980); (c) C. Higgs, K. A. Smith, G. B. McMillian, F. B. Dunning, and R. F. Stebbings, *J. Phys. B* **14**, L285 (1981); (d) R. F. Stebbings, F. B. Dunning, and C. Higgs, *J. Electron. Spectrosc. Relat. Phenom.* **23**, 333 (1981).
- ²⁴M. Matsuzawa, *Phys. Rev. A* **18**, 1396 (1978).
- ²⁵M. Matsuzawa, *Phys. Rev. A* **20**, 860 (1979).
- ²⁶H. S. W. Massey, *Rep. Prog. Phys.* **12**, 248 (1949).
- ²⁷The cross sections corresponding to the quantum-mechanical impulse approximation were calculated by using the formulas given by L. Petitjean and F. Gounand, *Phys. Rev. A* **30**, 2946 (1984). Note that the form factors used are those obtained by the binary encounter theory.
- ²⁸T. Yoshizawa and M. Matsuzawa, *J. Phys. Soc. Jpn.* **54**, 918 (1985).
- ²⁹F. B. Dunning (private communication).
- ³⁰Y. Hahn, *J. Phys. B* **14**, 985 (1981).
- ³¹M. Kimura and N. F. Lane, in *Advances in Atomic, Molecular, and Optical Physics*, edited by D. Bates and B. Bederson (Academic, New York, 1989), Vol. 26, p. 79.